Title

The NOTCH4–HEY1 Pathway Induces Epithelial–Mesenchymal Transition in Head and Neck Squamous Cell Carcinoma

Journal

Clinical Cancer Research, 24(3)

ISSN

1078-0432

Authors

Fukusumi, Takahito
Guo, Theresa W
Sakai, Akihiro
et al.

Publication Date

2018-02-01

DOI

10.1158/1078-0432.ccr-17-1366

Peer reviewed

HHS Public Access

Author manuscript

Clin Cancer Res. Author manuscript; available in PMC 2019 February 01.

Published in final edited form as:

Clin Cancer Res. 2018 February 01; 24(3): 619–633. doi:10.1158/1078-0432.CCR-17-1366.

The *NOTCH4-HEY1* pathway induces epithelial mesenchymal transition in head and neck squamous cell carcinoma

Takahito Fukusumi[1], **Theresa W Guo**[2], **Akihiro Sakai**[1], **Mizuo Ando**[1], **Shuling Ren**[1], **Sunny Haft**[1], **Chao Liu**[1], **Panomwat Amornphimoltham**[1], **J. Silvio Gutkind**[1], and **Joseph A Califano**[1]

[1]Moores Cancer Center, University of California San Diego, 3855 Health Science Drive, MC 0803 La Jolla, California 92093, U.S.A

[2]Department of Otolaryngology-Head and Neck Surgery, Johns Hopkins Medical Institutions, 1550 Orleans Street, Baltimore, Maryland 21231, U.S.A

Abstract

Background—Recently, several comprehensive genomic analyses demonstrated *NOTCH1* and *NOTCH3* mutations in head and neck squamous cell carcinoma (HNSCC) in approximately 20% of cases. Similar to other types of cancers, these studies also indicate that the *NOTCH* pathway is closely related to HNSCC progression. However, the role of *NOTCH4* in HNSCC is less well understood.

Methods—We analyzed *NOTCH4* pathway and downstream gene expression in the TCGA data set. To explore the functional role of *NOTCH4*, we performed *in vitro* proliferation, cisplatin viability, apoptosis, and cell cycle assays. We also compared the relationships among *NOTCH4, HEY1* and epithelial mesenchymal transition (EMT) related genes using the TCGA data set and *in vitro* assays.

Results—*HEY1* is specifically up-regulated in HNSCC compared with normal tissues in the TCGA data set. *NOTCH4* is more significantly related to *HEY1* activation in HNSCC in comparison to other *NOTCH* receptors. *NOTCH4* promotes cell proliferation, cisplatin resistance, inhibition of apoptosis, and cell cycle dysregulation. Furthermore, *NOTCH4* and *HEY1* up-regulation resulted in decreased *E-cadherin* expression and increased *Vimentin, Fibronectin*, *TWIST1*, and *SOX2* expression. *NOTCH4* and *HEY1* expression were associated with an EMT phenotypes as well as increased invasion and cell migration.

Conclusion—In HNSCC the *NOTCH4-HEY1* pathway is specifically up-regulated, induces proliferation and cisplatin resistance, and promotes EMT.

Keywords

Head and neck squamous cell carcinoma; TCGA; *NOTCH4*; *HEY1*; EMT

Correspondence: Joseph A. Califano, MD, Department of Otolaryngology - Head and Neck Surgery, University of California San Diego, 3855 Health Science Drive, MC 0803 La Jolla, California 92093, U.S.A. Phone: 619-543-7895; jcalifano@ucsd.edu.

Disclosure of Potential Conflict of Interest

The authors declare no potential conflicts of interest.

INTRODUCTION

Head and neck squamous cell carcinoma (HNSCC) is the sixth most common malignancy in the world (1). Despite recent medical progress, HNSCC prognosis has not dramatically improved (2). Thus, defining novel therapeutic target genes and pathways provide an opportunity to elucidate the molecular alterations associated with HNSCC mechanism and improve therapeutic design. Similar to other types of cancers, HNSCC develops through several steps, including the accumulation of genetic and epigenetic alterations, including *TP53* (3), *CDKN2A* (4), *EGFR* (5), and others.

The Cancer Genome Atlas (TCGA) project aims to examine genetic alterations for a better understanding of cancer pathology and, more importantly, identify signal pathways that can be used as potential targets in cancer treatment (6). Recently, using this data set, several types of cancers, such as lung (7), ovarian and colon cancer (8), were examined by comprehensive pathway analysis. For HNSCC, the comprehensive analysis of somatic genome alterations were also investigated using the TCGA data set (9). In this study, a *NOTCH* mutation was identified in approximately 20% of patients. In the other two articles, *NOTCH1* is the second most frequently mutated gene after *TP53* based on whole exome sequencing data (10, 11).

However, the *NOTCH* pathway changes its functional role depending on specific cancer site or histology. For example, an activated *NOTCH* pathway in cervical cancer has a poor prognosis (12). In the skin, a tumor suppressor function of *NOTCH* was reported in mouse keratinocyte tumor development (13). Interestingly, opposing and exclusive roles for the *NOTCH* pathway are reported in HNSCC (14). *NOTCH* pathway genes are up-regulated in HNSCC compared with normal or dysplasia tissues (15, 16). Sun *et al.* showed *NOTCH3* was overexpressed in HNSCC tumors compared with normal mucosa and *NOTCH1* wild type HNSCC had increased *NOTCH* downstream genes *HES1/HEY1* expression compared with normal mucosa, while *NOTCH1* mutated HNSCC do not show up-regulation (17). Inhibition of the *NOTCH* pathway via a γ-secretase inhibitor decreases cell proliferation and invasion (18). On the other hand, *NOTCH* mutations in HNSCC are considered as inactivating types, indicating that *NOTCH* has a tumor suppressor function (17, 19). For example, Grandis *et al.* showed that more *NOTCH1* gene mutations were observed than mutations in the other *NOTCH* receptor genes and many of *NOTCH1* mutations were missense type (17, 19). To further explore the role of specific *NOTCH* receptors, we examined alterations in *NOTCH* pathway genes associated with HNSCC compared with normal tissue using TCGA data sets, and found *NOTCH4-HEY1* pathway is specifically up-regulated in HNSCC. Furthermore, in this study we explore the functional role of the *NOTCH4-HEY1* pathway by using TCGA data set and *in vitro* experiments.

MATERIALS AND METHODS

TCGA data set

The mRNA expression data of the HNSCC patients were obtained from the TCGA data portal (http://tcga-data.nci.nih.gov/tcga/). We downloaded these data on 05/03/2016. These TCGA data included 520 HNSCC and 46 normal tissues. We used 447 HNSCC cases,

excluding 73 tumors with *NOTCH* mutations (Supplementary Table S1). *NOTCH* pathway genes included *DTX1, JAG1, JAG2, DLL1, DLL3, DLL4, NOTCH1, NOTCH2, NOTCH3, NOTCH4, POU5F1, SOX2, NANOG, CD44 and LMO2.* The *HES* high group was defined as tumors with expression 1 standard deviation greater than the mean of normal tissue for *HES1* or *HES5. HEY* and *NOTCH4* high groups were also defined as tumors with expression 1 standard deviation greater than the mean of normal tissue for *HEY1* and *NOTCH4*. Other samples were defined as a low expressing group. mRNA expression was log2-transformed to calculate fold-change. The clinical background and prognosis of these patients was obtained from the firebrowse web site (http://firebrowse.org/).

Cell culture

We used SKN3, Cal27, SCC61 and SCC090 HNSCC cell lines. SKN3 was obtained from the Japanese Collection of Research Bioresource (Ibaraki, Osaka, Japan). SCC61 was obtained from the Weichselbaum Laboratory at the University of Chicago. Cal27 and SCC090 cells were obtained from the Gutkind Laboratory at the University of California San Diego, Moores Cancer Center. SCC090 was established from Human Papilloma Virus (HPV)-positive HNSCC tissues. Other three cells are established from HPV-negative HNSCC tissues. SKN3 was cultured in RPMI-1640 medium (Sigma Aldrich, St. Louis, MO, U.S.A.). Cal27, SCC61 and SCC090 were cultured in Dulbecco's modified Eagle's medium (DMEM; Sigma Aldrich). Both mediums were supplemented with 10% fetal bovine serum (FBS) and a penicillin (50 U/ml) and streptomycin (50 μg/ml) cocktail. All cells were cultured under an atmosphere of 5% CO_2 at 37°C.

Quantitative real-time PCR

Quantitative real-time polymerase chain reaction (qRT-PCR) was used to validate siRNA-mediated knockdown of *NOTCH4* and *HEY1* and examine mRNA expression levels in each experiment. Briefly, total RNA was isolated from cells using the RNeasy plus mini kit (Qiagen, Hilden, Germany), and complementary DNA was synthesized using a high-capacity cDNA reverse transcription kit (Thermo Fisher Scientific, Waltham, MA, U.S.A.). We obtained all primers from TaqMan Gene Expression Assays (catalogue number: #4331182. Thermo Fisher Scientific). Each gene ID is described as follows: *β-actin (ACTB)*: Hs01060665_g1; *NOTCH4*: Hs00965895_g1; *HES1*: Hs00172878_m1; *HEY1*: Hs01114113_m1; *E-cadherin*: Hs01023895_m1; *Fibronectin*: Hs01549976_m1; *Vimentin*: Hs00958111_m1; *TWIST1*: Hs01675818_s1; *ALDH1*; Hs00946916_m1 and *SOX2*: Hs01053049_s1. The housekeeping gene *ACTB* was used as an internal control. qRT-PCR was performed using Quant Studio 6 Flex Real-Time PCR System (Thermo Fisher Scientific).

Western blotting

The following primary antibodies were added to nitrocellulose membrane with 5% non-fat dry milk in Tris-buffered saline and Tween 20: *NOTCH4* (#2423, Cell Signaling Technology, Danvers, MA, U.S.A.), *HES1* (#sc-25392, Santa Cruz, Dallas, TX, U.S.A.), *HEY1* (#ab22614, Abcam, Cambridge, MA, U.S.A.), *E-cadherin* (#610181, BD Bioscience, San Jose, CA, U.S.A.), *Fibronectin* (#ab2413, Abcam), *Vimentin* (#V6630, Sigma Aldrich), *TWIST1* (#sc-15393, Santa Cruz) and *SOX2* (#2748, Cell Signaling Technology). HRP

conjugated goat anti-mouse (#1010-05, 1:20,000 dilution; SouthernBiotech, Birmingham, AL, U.S.A.) or anti-rabbit antibodies (#4010-05, 1:20,000 dilution; SouthernBiotech) were used as secondary antibodies.

Si-RNA and sh-RNA

HNSCC cell lines were transfected with siRNA reagents using Lipofectamine RNAi MAX (Thermo Fisher Scientific) according to the manufacturer's instructions. All siRNA and si-control reagents used ON-TARGET plus siRNA reagents (GE Dharmacon, Lafayette, CO, U.S.A.). Each catalogue number is described as follows: si-*NOTCH4*: SMART pool ON-TARGET plus Human *NOTCH4* siRNA (L-011883-00-0005); si-*HES1*: SMART pool ON-TARGET plus Human *HES1* siRNA (L-007770-02-0005); si-*HEY1*: SMART pool ON-TARGET plus Human *HEY1* siRNA (L-008709-00-0005); and si-control: ON-TARGET plus Non-targeting Pool (D-001810-10-20). Medium was changed 16 hours after siRNA transfection. mRNA inhibition was observed at a concentration of 30 nM siRNA at 48 hours after transfection. We also used sh-control and sh-*NOTCH4* (CSHCTR001-LVRU6MP and HSH011877-LVRU6MP, Genecopoeia, Rockville, MD, U.S.A) to transfect Cal27 cells. The efficiency of down-regulation was validated by calculating mRNA and protein levels (Supplementary Fig. S2A,B, S3B,C,D,E,F). Thus, further analysis was performed under the same conditions.

Viability assay

Cells were seeded in 96-well plates at 1,500 to 9,000 cells/well. For proliferation assays, cell numbers were measured every 24 hours. For cisplatin viability assay, cells were cultured for 24 hours after seeding, and 0.1 to 81 μM cisplatin was added (EMD Millipore, Billerica, MA, U.S.A.). The viability was measured 72 hours after cisplatin exposure. All cell viabilities were measured using Vita Blue Cell Viability Reagent (bimake.com, Houston, TX, U.S.A.). After a 1.5-hour preincubation in the assay solution, the viable cell number in each well was calculated by the fluorescence (Ex = 530–570 nm, Em = 590–620 nm) as measured by a microplate reader (BioTek, Winooski, VT, U.S.A.). The assays were performed three or more times.

Flow cytometry analysis

All flow cytometry analysis such as the *NOTCH* activity, apoptosis, cell cycle and aldefluor assay were performed using BD FACSCalibur (BD Bioscience). *NOTCH* activity was examined using a pGreenFire1-Notch plasmid (#TR020PA-1, System Bioscience, Palo Alto, CA, U.S.A.). This lentiviral transfection was performed according to the manufacturer's protocol. The apoptotic cells were detected using Annexin V-FITC apoptosis detection kit (#C986X37, Sigma Aldrich). Cell cycle phase analysis was carried out using propidium iodide cell staining (#11348639001, Sigma Aldrich) and FlowJo software (ver.10, FLOWJO, Ashland, OR, U.S.A.). To assess *ALDH1* activity, we used aldefluor kit (#01700, STEMCELL Technologies, Vancouver, BC, Canada) at a concentration of 50 $\mu l ml^{-1}$. Diethylaminobenzaldehyde (DEAB) was used to inhibit *ALDH1* activity.

Sphere formation assay

Cells were seeded in 6-well ultra-low attachment culture dishes (Corning, Tewksbury, MA, U.S.A.) at 10,000 cells/well. Medium consisted of Repro Stem medium (ReproCELL, Yokohama, Japan) and basic fibroblast growth factor (bFGF: 5 ng/ml) without FBS. After 7 days, photos were obtained (Supplementary Fig. S3A), and sphere cells harvested to extract their mRNA. For qRT-PCR analysis, the adherent and sphere cells mRNA amounts are equalized. *NOTCH4* and *HEY1* expression were normalized by *ACTB* expression.

Migration and invasion assay

Migration assays were performed in cell culture insert (24-well 8μm pore size, #353097, Corning). The concentrations of cells were set from 10^5 to 2×10^5 cells/ml. Invasion assays were also performed in Corning BioCoat Matrigel invasion chambers (24-well 8μm pore size, #353097, Corning). The concentrations of cells were set from 2×10^5 to 4×10^5 cells/ml. Cells were seeded on uncoated or Matrigel-coated inserts in 500 ml of serum-free medium for migration or invasion assays respectively. The lower chambers were filled with 750 μl of 10% FBS-supplemented medium. After 48 h, the cells on the lower surface of the insert were fixed and stained with crystal violet. The number of stained cells was counted at more than three fields under a microscope.

Statistical analysis

All *in vitro* experiments were performed at least three times. The statistical comparisons of two groups were performed using the Student's *t*-test. The TCGA data set analysis of *NOTCH* pathway genes in the *HES* and *HEY* high and low groups was adjusted by false discovery rate using the Benjamini–Hochberg method. Clinical status was compared between two groups using Pearson's chi-square test. Overall survival was compared using Log-Rank test. Differences were considered significant when $P < 0.05$. All statistical analyses were performed using JMP 12 software (SAS, Cary, NC, U.S.A.).

RESULTS

NOTCH4-HEY1 is upregulated in HNSCC

First, we examined which *NOTCH* pathway genes were significantly related *NOTCH* pathway activation in HNSCC compared with normal tissue using TCGA data sets. We excluded 73 *NOTCH* mutant samples (Supplementary Table S1). Thus, we examined 447 HNSCC and 46 normal tissues. The *NOTCH* downstream genes *HES1/5* and *HEY1* were selected as indicators of downstream *NOTCH* activity. Two groups were divided according the mRNA expression of these genes compared with normal tissues. No significant difference in *NOTCH* pathway genes was noted between the *HES1/5* high and low groups. On the other hand, *HEY1* expression exhibited a significant correlation with several *NOTCH* pathway genes (*DLL4, NOTCH1, NOTCH2, NOTCH3, NOTCH4*, and *SOX2*). All *NOTCH* receptors were significantly related to *HEY*1 expression (Supplementary Fig. S1A). Among these receptors, *NOTCH4* exhibited the most significant correlation to *HEY1* overexpression. *NOTCH4* expression in the *HEY1* high expressing group was increased approximately 1.58–fold compared with the *HEY1* low expressing group (Fig. 1A,

Supplementary Fig. S1A). We also compared *HES1, HES5* and *HEY1* expression between HNSCC and normal tissues using the TCGA data set. *HES1* expression in HNSCC was significantly decreased compared with normal tissues ($P = 0.0002$). *HES5* expression was not significantly different between HNSCC and normal tissues ($P = 0.1251$). On the other hand, *HEY1* expression of HNSCC significantly increased compared with normal tissues ($P < 0.0001$). *HEY1* expression in tumor samples was about two times more than that of normal samples (Fig. 1B). In summary, *HEY1* was up-regulated compared with normal tissues and was most related to *NOTCH4* among the *NOTCH* receptors in HNSCC. These results suggested that the *NOCH4-HEY1* pathway was specifically up-regulated in *NOTCH* wild type HNSCC compared with normal tissue.

NOTCH4 inhibition inhibits HNSCC and sensitizes HNSCC to cisplatin

To elucidate the properties of the *NOTCH4-HEY1* pathway in HNSCC cells, we examined *NOTCH4* function in HNSCC cells. First, we examined how *NOTCH* activity was affected by si-*NOTCH4* cells (Supplementary Fig. S2A, S2B) using pGreenFire1-Notch plasmid. This reporter vector shows increased *NOTCH* activity (GFP+) cells as a result of GFP expression under the binding of a *NOTCH* specific transcriptional response element (Fig. 2A). Using this vector, we showed si-*NOTCH4* cells significantly decreased *NOTCH* activity in all cell lines (Fig. 2B, Supplementary Fig. S2C). We also compared cell proliferation between si-control and si-*NOTCH4* (Fig. 2C). Si-*NOTCH4* cells significantly reduced their proliferation compared with si-control cells in all cell lines. In SCC090 cells, si-*NOTCH4* cell numbers decreased from day 2 to 3. Compared with si-control, si-*NOTCH4* cell numbers were decreased by 20~40% on day 3 (SKN3: 33.3%; Cal27: 24.9%; SCC61: 42.0%; SCC090: 37.5%). Next, we assessed the chemo-resistance properties of si-*NOTCH4* cells (Fig. 2D, Supplementary Fig. S2D). We used cisplatin, commonly used for HNSCC chemotherapy. Similar to proliferation assays, si-*NOTCH4* cells significantly decreased their cisplatin resistance compared with si-control cells in all cell lines. In comparing IC50, significant differences were noted between the si-control and si-*NOTCH4*. In particular, Cal27, SCC61 and SCC090 cells decreased IC50 by half to a third (Fig. 2D). These results demonstrated that *NOTCH4* inhibition affects *NOTCH* activity, cell proliferation, and enhances chemo sensitivity in HNSCC cells.

NOTCH4 inhibits apoptosis and alters cell cycle

To elucidate what mechanism decreases si-*NOTCH4* cell proliferation, we assumed it related to apoptosis and cell cycle alteration. First, we performed apoptosis assays (Supplementary Fig. S2E) and found that all the si-*NOTCH4* cells statistically increased the apoptotic cell fraction compared to si-control cells in a modest fashion (Fig. 2E). Furthermore, we performed cell cycle analysis in si-*NOTCH4* cells (Supplementary Fig. S2F). The significant increase of G0/G1 phase and decrease of S phase was noted in si-*NOTCH4* cells. This result suggested that the si-*NOTCH4* cells inhibited cell cycle progression compared to si-control cells (Fig 2F). In these results, we can indicate that *NOTCH4* decreases cell proliferation by regulating both apoptosis and cell cycle.

NOTCH4 expression is correlated to EMT related gene expression

We explored other mechanisms related to *NOTCH4* and HNSCC properties. *NOTCH4* has been noted to induce epithelial mesenchymal transition (EMT) in melanoma (20). EMT promotes cancer proliferation (21) and can be associated with chemo-resistance (22). Thus, we hypothesized that *NOTCH4* is also related to EMT in HNSCC and examined the relationship between *NOTCH4* and EMT-related genes. Using the TCGA data set, we compared EMT related genes expression between *NOTCH4* high and low groups. A significant decrease in the expression of *E-cadherin*, an epithelial marker, was noted in the *NOTCH4* high group compared with the low group ($P = 0.001$, ratio = 0.760). The expression of mesenchymal markers, such as *N-cadherin, Vimentin*, and *Fibronectin*, was significantly increased in the high group compared with the low group ($P < 0.0001$). The expression of mesenchymal markers of *NOTCH4* high group was several times higher than that of low group (*N-cadherin*: 2.854, *Vimentin*: 1.937, *Fibronectin*: 3.266). *TWIST1* is known as an EMT-inducing gene, and its expression was significantly increased in the high group ($P < 0.0001$). The *TWIST1* expression of *NOTCH4* high group was 1.749 times more than that of *NOTCH4* low group (Fig. 3A). *SOX2* expression is also related to EMT genes (23). Its expression was also significantly increased in the high group ($P < 0.0046$). The *SOX2* expression of *NOTCH4* high group was 1.609 times more than that of *NOTCH4* low group by using Student's *t*-test (Fig. 3A). These results show an association between *NOTCH4* and EMT in HNSCC and raise the possibility that *NOTCH4* activation may in part drive EMT in HNSCC.

NOTCH4 promotes HNSCC EMT

To confirm this TCGA data set analysis *in vitro*, we generated sphere colonies (Supplementary Fig. S3A) that were employed to induce enrichment of EMT-related gene expression (24). As noted, the *NOTCH4* expression was significantly increased in sphere cells derived from all HNSCC cell lines examined. *NOTCH4* expression in sphere cells was increased approximately 1.8- to 3.5–fold compared with parental cells (Fig. 3B). Next, we also compared EMT-related genes between si-*NOTCH4* and si-control cells. si-*NOTCH4* cells significantly increased *E-cadherin* expression in SKN3, Cal27 and SCC61 cells. On the contrary, si-*NOTCH4* significantly reduced *Vimentin* (in Cal27, SCC61 and SCC090), *Fibronectin* (in the all cell lines) and *TWIST1* (in Cal27, SCC61 and SCC090) expression. The *SOX2* expressions of si-*NOTCH4* cells significantly decreased in Cal27, SCC61 and SCC090 cells. However, a portion of si-*NOTCH4* cells did not have significant changes in EMT-related genes. For example, *E-cadherin* and *TWIST1* expression did not exhibit significant differences between si-*NOTCH4* and si-control cells in SKN3 and SCC090, respectively. *Fibronectin* expression in si-*NOTCH4* cells was significantly increased compared with si-control Cal27 cells. *SOX2* expression in si-*NOTCH4* cells was also significantly increased compared with si-control SKN3 cells (Fig. 4A). In western blot experiments, elevated *E-cadherin* expression was also found in Cal27 si-*NOTCH4* cells. But, there was no obvious difference of *E-cadherin* expression between SKN3 si-control and si-*NOTCH4* cells. *Fibronectin, Vimentin, TWIST1* and *SOX2* expression decreased in both SKN3 and Cal27 si-*NOTCH4* cells (Fig. 4B). Next, we examined the function of another HNSCC specific *NOTCH* pathway gene, *HEY1*.

NOTCH4 specifically promotes *HEY1* expression in HNSCC

Our TCGA data set analysis showed no significant difference in *NOTCH* pathway genes between the *HES* high and low expressing tumors. On the other hand, *HEY1* expression exhibited a significant correlation with several *NOTCH* pathway genes (Fig. 1A, and Supplementary Fig. S1A). To confirm these findings *in vitro*, *HES1* and *HEY1* expression were compared between si-control and si-*NOTCH4* by using qRT-PCR. No significant differences of *HES1* expression were noted between si-control and si-*NOTCH4* in SKN3, SCC61, and SCC090. In Cal27, *HES1* expression was significantly increased in si-*NOTCH4* (Fig. 5A). On the other hand, *HEY1* expression was significantly decreased in all cell lines with si-*NOTCH4* (Fig. 5B). In western blot experiments, we obtained similar results. There were no *HES1* expression changes between si-control and si-*NOTCH4* cells, but si-*NOTCH4* cells had less *HEY1* expression than si-control cells (Fig. 5C). Thus, similar to the TCGA data set analysis, our *in vitro* experiments also showed that *NOTCH4* was significantly associated with *HEY1* expression.

HEY1 inhibition decreases *NOTCH4* expression in HNSCC

HEY1 is generally activated by *NOTCH* receptors. However, si-*HEY1* cells significantly decreased *NOTCH4* mRNA expression in all HNSCC cell lines (Fig. 5D and Supplementary Fig. S3B, S3C). We also found less *NOTCH4* expression in si-*HEY1* cells of SKN3, Cal27 and SCC61 by western blot (Fig. 5E). These results may indicate that *HEY1* also reciprocally regulates *NOTCH4* expression in HNSCC.

HEY1 is expression is associated with EMT genes in HNSCC

Next, we hypothesized that *HEY1* was also related to EMT in HNSCC similar to *NOTCH4*. Thus, using a TCGA data set similar to that used for *NOTCH4* analysis, EMT-related genes were compared between *HEY1* high and low groups (Fig. 6A). In contrast to *NOTCH4*, *E-cadherin* expression was not significantly decreased in the *HEY1* high group ($P = 0.10$, ratio = 0.825). However, the expressions of *N-cadherin* ($P = 0.0038$), *Vimentin* ($P = 0.0068$), *Fibronectin* ($P = 0.0002$), *TWIST1* ($P = 0.0025$), and *SOX2* ($P < 0.0001$) were significantly increased in the *HEY1* high group (Fig. 6A). The expression of other EMT related genes of *HEY1* high group were several times more than that of low group (*N-cadherin*: 2.332, *Vimentin*: 1.249, *Fibronectin*: 1.720, *TWIST1*: 1.228, *SOX2*: 3.724).

Similar to the previous *NOTCH4* experiment, we compared *HEY1* expression between parental and sphere cells. *HEY1* expression significantly increased in sphere cells of all HNSCC cell lines. *HEY1* expression in sphere cells was increased approximately 1.4- to 3.5–fold compared with parental cells (Fig. 6B). To summarize our sphere cells experiments as shown Fig. 3B and 6B, sphere cells were enriched in both *NOTCH4* and *HEY1* expression.

We also ascertained the relation of *HEY1* and EMT genes *in vitro*. As shown in Fig. 7A, si-*HEY1* cells significantly increased *E-cadherin* expression in the all cell lines. On the contrary, si-*NOTCH4* significantly reduced *Vimentin, Fibronectin* and *TWIST1* expression in the all cell lines. The *SOX2* expressions of si-*HEY1* cells significantly decreased in SKN3, SCC61 and SCC090 cells. However, only si-*HEY1* Cal27 cells did not have

significant changes of *SOX2* expression (Fig. 7A). In western blot experiments, we also noted that si-*HEY1* cells had higher *E-cadherin* expression and less mesenchymal marker gene (*Vimentin, Fibronectin, TWIST1* and *SOX2*) expression than si-control cells. Only Cal27 cells lacked an obvious difference of *E-cadherin* expression (Fig. 7B). Furthermore, to assess whether these expression changes affect the cell phenotype, we performed migration and invasion assays. We found significant decrease of migrated and invaded cells in si-*NOTCH4* and si-*HEY1* cells compared to si-control cells (Fig. 7C, 7D and 7E). In these results, we concluded that the *NOTCH4-HEY1* pathway induces EMT in HNSCC.

Stable transfectants using sh-*NOTCH4* were created in Cal27 cells, however, despite RNA knockdown, protein levels of *NOTCH4* were unchanged, indicating that *NOTCH4* expression is obligate for survival in cell line systems (Supplementary Fig. S3D, S3E, S3F).

DISCUSSION

The *NOTCH* pathway is highly conserved through evolution and plays important roles during embryonic development (25). The *NOTCH* pathway also affects normal tissue cell proliferation and inhibits apoptosis (26). In mammals, the *NOTCH* pathway has four receptors (*NOTCH1, 2, 3 and 4*) and five ligands (*JAG1* and *2, DLL1, 3* and *4*), all of which are type 2 transmembrane proteins (27). This pathway is activated by a ligand binding to a *NOTCH* receptor. Subsequently, the γ-secretase complex releases the intracellular domain of the *NOTCH* receptor, which moves to the nucleus, resulting in the transcriptional activation of *NOTCH* target genes, such as the *HES/HEY* family (27, 28).

The *NOTCH* pathway is also an attractive cancer therapeutic target. For instance, inhibition of the *NOTCH* pathway by the γ-secretase inhibitor (GSI) decreases cell proliferation and invasion (18). Thus, several clinical trials use GSI for cancer treatment (29–32). However, GSI exhibits toxicity in normal stem cells and clinically results in gastrointestinal toxicity, diarrhea, hepatotoxicity and nephrotoxicity (33–37). Wu *et al.* considered that these adverse events resulted from GSI nonspecific effect for *NOTCH* pathway. Thus, they showed that inhibition of *NOTCH1* or *NOTCH2* alone mildly affected intestinal morphology and some goblet cell metaplasia, but that inhibition of both *NOTCH1* and *2* caused severe intestinal toxicity in their mouse model (36). Furthermore, many studies assumed that GSIs used for clinical trails have biological equivalent effect for each *NOTCH* receptors. But, Ran *et al.* examined the *NOTCH* inhibition potential of several GSIs and showed these GSIs had different effect for each *NOTCH* receptors. For instance, not all GSIs had sufficient pharmacological effect for *NOTCH4* (38). Harrison *et al.* also showed that two GSIs (DAPT and Dibenzazepine) had no effect on *NOTCH4* in breast cancer cells (39).

Our TCGA data set analysis showed that that only *HEY1* is up-regulated among the *NOTCH* downstream genes compared with normal tissues, in addition *NOTCH4* is the most significantly associated with *HEY1* activation in HNSCC. Next, we used pGreenFire1-Notch plasmid in order to examine to what extent *NOTCH4* related to *NOTCH* activity. Wicha *et al.* used this vector to assess the *NOTCH* activity and show that *NOTCH* activity is related to tumorigenicity, cancer stem cells (CSCs), and poor prognosis in lung adenocarcinoma and breast cancer (40, 41). *NOTCH4* receptor was expressed at 3-5 fold higher levels in the

NOTCH high activity cells compared to *NOTCH* low activity breast cancer cell lines. (41). We also show that si-*NOTCH4* cells significantly decreased *NOTCH* activity in all cell lines. *NOTCH4* is known to promote mouse mammary epithelial transformation and tumorigenesis (42). This report is the first study linking *NOTCH4* and a cancer phenotype. Soriano *et al.* also demonstrated that normal mammary cells exhibited altered shape and promoted an invasive and tumorigenic phenotype by *NOTCH4* (43). Thus, we next examined *NOTCH4* function in HNSCC and showed *NOTCH4* affected HNSCC cell proliferation and cisplatin resistance *in vitro.* There are several papers indicates that the *NOTCH* pathway affects cell cycle and apoptosis. For instance, Demarest *et al.* indicates that the *NOTCH* pathway promotes cell cycle progression and inhibits apoptosis by using T-ALL cells (44). As a result of our apoptosis and cell cycle analysis, we can suggest that *NOTCH4* decreases cell growth by regulating both apoptosis and the cell cycle.

Lombardo *et al.* showed that the EMT phenotype was induced by *NOTCH4* in breast cancer cells (45). *NOTCH4* is also known as an EMT trigger and promotes the metastasis of melanoma cells (20). EMT promotes cancer migration, invasion, metastasis (46) and is also related to poor prognosis. Thus, EMT represents one of the most important phenotypes in cancer therapy. In the melanoma study, *NOTCH4* was also related to *SOX2* expression and cell invasion. Clinically, approximately 60% of melanoma tissues express high levels of *NOTCH4* protein. High *NOTCH4* expression is related to metastasis and poor prognosis (20). We also demonstrated that *NOTCH4* was related to EMT gene expression in HNSCC using the TCGA data set. By qRT-PCR and western blot analysis, not all cell lines exhibited a significant change in EMT-related genes upon *NOTCH4* knockdown.

Using the TCGA data set, we demonstrated that *HEY1* was significantly up-regulated in tumors compared with normal tissue among the *NOTCH* downstream genes. qRT-PCR and western blot analysis revealed the same result. In general, *HEY1* is related to the development of the heart, neurogenesis and osteogenesis (47–51). In cardiovascular studies, *HEY1* regulates endocardia EMT in septum and valve development (52). In heart development, *HEY1* cooperates with *TWIST1* to promote EMT (53). In cancer studies, *HEY1* is an indicator of poor clinical prognosis in several cancer types, such as pancreas (54), colon (55), esophagus (56), and thyroid (57). In a thyroid cancer study, *HEY1* expression was also related to recurrence and metastasis (57). Lung metastasis of osteosarcoma cells was also promoted by *HEY1* in a nude mouse model (58). However, few studies about EMT and *HEY1* in cancers have been performed. Our current study is the first HNSCC study that assesses the relationship between *HEY1* and EMT. In the TCGA data set analysis, *TWIST1* and mesenchymal genes such as *N-cadherin, Vimentin* and *Fibronectin* were significantly increased in the *HEY1* high group. But, *E-cadherin* expression was not significantly decreased in the *HEY1* high group (Fig. 6A). However, this finding may result from the method used to divide the groups. For example, if the group was divided by the average of HNSCC *HEY1* expression, *E-cadherin* had significant differences similar to other EMT-related genes (Supplementary Fig. S4A). Furthermore, our *in vitro* experiments showed that *E-cadherin, Vimentin, Fibronectin* and *TWIST1* expressions exhibit significant differences between si-*HEY1* and si-control cells in all cell lines. We also revealed that the *NOTCH4-HEY1* pathway was significantly correlated with *SOX2* in the TCGA data set and *in vitro*. *SOX2* is a marker gene of tissue stem cells (59), CSCs (60) as well as EMT (23) in

the head and neck region. Furthermore, *SOX2* is reported to co-expressed with *HEY1/HEY2* in the inner ear (61) and regulated by the *NOTCH* pathway in the developing inner ear. During inner ear development, *HEY1* expression is significantly increased in the regulation of *SOX2* (62). The *NOTCH* pathway is also necessary to maintain *SOX2*-positive stem cells in the pituitary gland (63). In our TCGA results, the *HEY1* high group exhibited 3.72–fold increased *SOX2* expression (Fig. 6A). In *in vitro* experiments, inhibition of *HEY1* resulted in significantly decreased *SOX2* expression. In these contexts, we suggest that *HEY1* may regulate *SOX2* as well as other EMT related genes in HNSCC (Fig. 7A, 7B). EMT is known to enhance cell migration and invasion (64). We also showed that both *NOTCH4* and *HEY1* promoted migration and invasion properties (Fig. 7C, 7D and 7E). Thus, we concluded that the *NOTCH4–HEY1* pathway induces EMT in HNSCC.

NOTCH4 expression is also reported to increase in breast CSCs (65). EMT is closely correlated with CSCSs (66). In HNSCC, *CD10* (67), *CD44* (68) and *ALDH1* (69) are defined as CSCs markers. Thus, the expressions of these markers were compared between *NOTCH4* and *HEY1* high/low groups using the TCGA data set. Significant differences in *ALDH1* and *CD10* but not *CD44* expression were noted between *NOTCH4* high and low groups (Supplementary Fig. S5A). The *ALDH1* expression also significantly increased in the *HEY1* high group compared with the *HEY1* low group. *CD10* and *CD44* expression did not exhibit a significant difference between *HEY1* high and low groups (Supplementary Fig. S5B). Regarding *ALDH1* expression, the *NOTCH4* high group exhibited 1.63-fold increased expression and the *HEY1* high group exhibited 5.87-fold increased expression compared with each low group. To elucidate the relationships between *NOTCH4-HEY1* and *ALDH1 in vitro*, *ALDH1* expression was compared by using qRT-PCR, and significantly increased in both si-*NOTCH4* and si-*HEY1* of all HNSCC cell lines except Cal27 si-*NOTCH4* cells (Supplementary Fig. S5C). We also performed aldefluor assays and found similar results, with both si-*NOTCH4* and si-*HEY1* cells showing and increased *ALDH1*+ fraction (Supplementary Fig. S5D, S5E). Young *et al.* show *ALDH1* regulates *NOTCH1* expression in ovarian cancer cells (70). In our results, we also suggest that *ALDH1* can regulate *NOTCH4-HEY1* pathway.

Wicha *et al.* showed high *NOTCH4* and *HEY1* expression in primary breast cancer patient samples correlated with poor overall survival using a TCGA data set (41). Simões *et al.* also showed *NOTCH4* high breast cancer had high *HEY1* expression and worse clinical prognosis, such as overall survival and metastasis free survival (65). Thus, we also compared the clinical background and prognosis between the *NOTCH4/HEY1* high and low group using a TCGA data set (Supplementary Fig. S6A, S6B and Supplementary Table S2). We noted is no significant difference between the *NOTCH4/HEY1* high and low group except the age of the *HEY1* high/low group (Supplementary Table S2), as well as no difference in overall survival between the *NOTCH4/HEY1* high and low group. (Supplementary Fig. S6A, S6B).

HEY1 is generally activated by *NOTCH* receptors. However, we demonstrate that si-*HEY1* cells significantly decreased *NOTCH4* expression in all HNSCC cell lines (Fig. 5D, 5E). Whether this effect is direct or indirect is not known; however, this result may indicate that

HEY1 also regulates *NOTCH4* expression. In other words, the *NOTCH4-HEY1* pathway may create a positive feedback loop in HNSCC.

In this study, we used one HPV-positive HNSCC cell line, SCC090. The gene expression and pathways of HPV-positive HNSCC differs from HPV-negative HNSCC (71, 72). Regarding cancer therapy, HPV-positive HNSCC is more sensitive to radiation and chemotherapy than HPV-negative cancer (73). However, in our experiments, there were no differences in the results between SCC090 and the other HPV-negative HNSCC cell lines. This finding indicates that the function of the *NOTCH4-HEY1* pathway does not change regardless of HPV status.

In conclusion, we demonstrate that the *NOTCH4-HEY1* pathway of HNSCC is specifically up-regulated and promotes EMT. *NOTCH4* is also related to proliferation, chemoresistance, apoptosis inhibition, and cell cycle alteration in HNSCC. Thus, this pathway may represent a novel target for HNSCC therapy or may serve as a target to improve chemotherapeutic sensitivity.

Supplementary Material

Refer to Web version on PubMed Central for supplementary material.

Acknowledgments

Financial Support

This study was supported by National Institute of Dental and Craniofacial Research (NIDCR, number: R01DE023347). J.A.Califano received this grant.

References

1. Argiris A, Karamouzis MV, Raben D, Ferris RL. Head and neck cancer. The Lancet. 2008; 371:1695–709.
2. Lo WL, Kao SY, Chi LY, Wong YK, Chang RC. Outcomes of oral squamous cell carcinoma in Taiwan after surgical therapy: factors affecting survival. J Oral Maxillofac Surg. 2003; 61:751–8. [PubMed: 12856245]
3. Poeta ML, Manola J, Goldenberg D, Forastiere A, Califano JA, Ridge JA, et al. The Ligamp TP53 Assay for Detection of Minimal Residual Disease in Head and Neck Squamous Cell Carcinoma Surgical Margins. Clin Cancer Res. 2009; 15:7658–65. [PubMed: 19996217]
4. Demokan S, Chuang A, Suoglu Y, Ulusan M, Yalniz Z, Califano JA, et al. Promoter methylation and loss of p16(INK4a) gene expression in head and neck cancer. Head Neck. 2012; 34:1470–5. [PubMed: 22106032]
5. Bonner JA, Harari PM, Giralt J, Cohen RB, Jones CU, Sur RK, et al. Radiotherapy plus cetuximab for locoregionally advanced head and neck cancer: 5-year survival data from a phase 3 randomised trial, and relation between cetuximab-induced rash and survival. Lancet Oncol. 2010; 11:21–8. [PubMed: 19897418]
6. de Castro G Jr, Negrao MV. The Cancer Genome Atlas findings in head and neck cancer: a renewed hope. Curr Opin Oncol. 2014; 26:245–6. [PubMed: 24709977]
7. Comprehensive genomic characterization of squamous cell lung cancers. Nature. 2012; 489:519–25. [PubMed: 22960745]
8. Dellinger AE, Nixon AB, Pang H. Integrative Pathway Analysis Using Graph-Based Learning with Applications to TCGA Colon and Ovarian Data. Cancer Inform. 2014; 13:1–9.

9. Cancer Genome Atlas N. Comprehensive genomic characterization of head and neck squamous cell carcinomas. Nature. 2015; 517:576–82. [PubMed: 25631445]
10. Agrawal N, Frederick MJ, Pickering CR, Bettegowda C, Chang K, Li RJ, et al. Exome sequencing of head and neck squamous cell carcinoma reveals inactivating mutations in NOTCH1. Science. 2011; 333:1154–7. [PubMed: 21798897]
11. Stransky N, Egloff AM, Tward AD, Kostic AD, Cibulskis K, Sivachenko A, et al. The mutational landscape of head and neck squamous cell carcinoma. Science. 2011; 333:1157–60. [PubMed: 21798893]
12. Yousif NG, Sadiq AM, Yousif MG, Al-Mudhafar RH, Al-Baghdadi JJ, Hadi N. Notch1 ligand signaling pathway activated in cervical cancer: poor prognosis with high-level JAG1/Notch1. Arch Gynecol Obstet. 2015; 292:899–904. [PubMed: 25842263]
13. Dotto GP. Notch tumor suppressor function. Oncogene. 2008; 27:5115–23. [PubMed: 18758480]
14. Yap LF, Lee D, Khairuddin A, Pairan MF, Puspita B, Siar CH, et al. The opposing roles of NOTCH signalling in head and neck cancer: a mini review. Oral Dis. 2015; 21:850–7. [PubMed: 25580884]
15. Hijioka H, Setoguchi T, Miyawaki A, Gao H, Ishida T, Komiya S, et al. Upregulation of Notch pathway molecules in oral squamous cell carcinoma. Int J Oncol. 2010; 36:817–22. [PubMed: 20198324]
16. Lee SH, Hong HS, Liu ZX, Kim RH, Kang MK, Park NH, et al. TNFalpha enhances cancer stem cell-like phenotype via Notch-Hes1 activation in oral squamous cell carcinoma cells. Biochem Biophys Res Commun. 2012; 424:58–64. [PubMed: 22728043]
17. Sun W, Gaykalova DA, Ochs MF, Mambo E, Arnaoutakis D, Liu Y, et al. Activation of the NOTCH pathway in head and neck cancer. Cancer Res. 2014; 74:1091–104. [PubMed: 24351288]
18. Yao J, Duan L, Fan M, Wu X. Gamma-secretase inhibitors exerts antitumor activity via down-regulation of Notch and Nuclear factor kappa B in human tongue carcinoma cells. Oral Dis. 2007; 13:555–63. [PubMed: 17944672]
19. Egloff AM, Grandis JR. Molecular pathways: context-dependent approaches to Notch targeting as cancer therapy. Clin Cancer Res. 2012; 18:5188–95. [PubMed: 22773520]
20. Lin X, Sun B, Zhu D, Zhao X, Sun R, Zhang Y, et al. Notch4+ cancer stem-like cells promote the metastatic and invasive ability of melanoma. Cancer Sci. 2016; 107:1079–91. [PubMed: 27234159]
21. Thiery JP. Epithelial-mesenchymal transitions in tumour progression. Nat Rev Cancer. 2002; 2:442–54. [PubMed: 12189386]
22. Saxena M, Stephens MA, Pathak H, Rangarajan A. Transcription factors that mediate epithelial-mesenchymal transition lead to multidrug resistance by upregulating ABC transporters. Cell Death Dis. 2011; 2:e179. [PubMed: 21734725]
23. Yang N, Hui L, Wang Y, Yang H, Jiang X. Overexpression of SOX2 promotes migration, invasion, and epithelial-mesenchymal transition through the Wnt/beta-catenin pathway in laryngeal cancer Hep-2 cells. Tumour Biol. 2014; 35:7965–73. [PubMed: 24833089]
24. Han XY, Wei B, Fang JF, Zhang S, Zhang FC, Zhang HB, et al. Epithelial-mesenchymal transition associates with maintenance of stemness in spheroid-derived stem-like colon cancer cells. PLoS One. 2013; 8:e73341. [PubMed: 24039918]
25. Bray SJ. Notch signalling: a simple pathway becomes complex. Nat Rev Mol Cell Biol. 2006; 7:678–89. [PubMed: 16921404]
26. Artavanis-Tsakonas S, Rand MD, Lake RJ. Notch signaling: cell fate control and signal integration in development. Science. 1999; 284:770–6. [PubMed: 10221902]
27. Gordon WR, Arnett KL, Blacklow SC. The molecular logic of Notch signaling–a structural and biochemical perspective. J Cell Sci. 2008; 121:3109–19. [PubMed: 18799787]
28. Aster JC, Pear WS, Blacklow SC. Notch signaling in leukemia. Annu Rev Pathol. 2008; 3:587–613. [PubMed: 18039126]
29. Strosberg JR, Yeatman T, Weber J, Coppola D, Schell MJ, Han G, et al. A phase II study of RO4929097 in metastatic colorectal cancer. Eur J Cancer. 2012; 48:997–1003. [PubMed: 22445247]

30. De Jesus-Acosta A, Laheru D, Maitra A, Arcaroli J, Rudek MA, Dasari A, et al. A phase II study of the gamma secretase inhibitor RO4929097 in patients with previously treated metastatic pancreatic adenocarcinoma. Invest New Drugs. 2014; 32:739–45. [PubMed: 24668033]
31. Lee SM, Moon J, Redman BG, Chidiac T, Flaherty LE, Zha Y, et al. Phase 2 study of RO4929097, a gamma-secretase inhibitor, in metastatic melanoma: SWOG 0933. Cancer. 2015; 121:432–40. [PubMed: 25250858]
32. Chen X, Gong L, Ou R, Zheng Z, Chen J, Xie F, et al. Sequential combination therapy of ovarian cancer with cisplatin and gamma-secretase inhibitor MK-0752. Gynecol Oncol. 2016; 140:537–44. [PubMed: 26704638]
33. Searfoss GH, Jordan WH, Calligaro DO, Galbreath EJ, Schirtzinger LM, Berridge BR, et al. Adipsin, a biomarker of gastrointestinal toxicity mediated by a functional gamma-secretase inhibitor. J Biol Chem. 2003; 278:46107–16. [PubMed: 12949072]
34. van Es JH, van Gijn ME, Riccio O, van den Born M, Vooijs M, Begthel H, et al. Notch/gamma-secretase inhibition turns proliferative cells in intestinal crypts and adenomas into goblet cells. Nature. 2005; 435:959–63. [PubMed: 15959515]
35. Garber K. Notch emerges as new cancer drug target. J Natl Cancer Inst. 2007; 99:1284–5. [PubMed: 17728207]
36. Wu Y, Cain-Hom C, Choy L, Hagenbeek TJ, de Leon GP, Chen Y, et al. Therapeutic antibody targeting of individual Notch receptors. Nature. 2010; 464:1052–7. [PubMed: 20393564]
37. Purow B. Notch inhibition as a promising new approach to cancer therapy. Adv Exp Med Biol. 2012; 727:305–19. [PubMed: 22399357]
38. Ran Y, Hossain F, Pannuti A, Lessard CB, Ladd GZ, Jung JI, et al. gamma-Secretase inhibitors in cancer clinical trials are pharmacologically and functionally distinct. EMBO Mol Med. 2017; 9:950–66. [PubMed: 28539479]
39. Harrison H, Farnie G, Howell SJ, Rock RE, Stylianou S, Brennan KR, et al. Regulation of breast cancer stem cell activity by signaling through the Notch4 receptor. Cancer Res. 2010; 70:709–18. [PubMed: 20068161]
40. Hassan KA, Wang L, Korkaya H, Chen G, Maillard I, Beer DG, et al. Notch pathway activity identifies cells with cancer stem cell-like properties and correlates with worse survival in lung adenocarcinoma. Clin Cancer Res. 2013; 19:1972–80. [PubMed: 23444212]
41. D'Angelo RC, Ouzounova M, Davis A, Choi D, Tchuenkam SM, Kim G, et al. Notch reporter activity in breast cancer cell lines identifies a subset of cells with stem cell activity. Mol Cancer Ther. 2015; 14:779–87. [PubMed: 25673823]
42. Gallahan D, Callahan R. The mouse mammary tumor associated gene INT3 is a unique member of the NOTCH gene family (NOTCH4). Oncogene. 1997; 14:1883–90. [PubMed: 9150355]
43. Soriano JV, Uyttendaele H, Kitajewski J, Montesano R. Expression of an activated Notch4(int-3) oncoprotein disrupts morphogenesis and induces an invasive phenotype in mammary epithelial cells in vitro. Int J Cancer. 2000; 86:652–9. [PubMed: 10797286]
44. Demarest RM, Ratti F, Capobianco AJ. It's T-ALL about Notch. Oncogene. 2008; 27:5082–91. [PubMed: 18758476]
45. Lombardo Y, Faronato M, Filipovic A, Vircillo V, Magnani L, Coombes RC. Nicastrin and Notch4 drive endocrine therapy resistance and epithelial to mesenchymal transition in MCF7 breast cancer cells. Breast Cancer Res. 2014; 16:R62. [PubMed: 24919951]
46. Kang Y, Massague J. Epithelial-mesenchymal transitions: twist in development and metastasis. Cell. 2004; 118:277–9. [PubMed: 15294153]
47. Sakamoto M, Hirata H, Ohtsuka T, Bessho Y, Kageyama R. The basic helix-loop-helix genes Hesr1/Hey1 and Hesr2/Hey2 regulate maintenance of neural precursor cells in the brain. J Biol Chem. 2003; 278:44808–15. [PubMed: 12947105]
48. Kokubo H, Miyagawa-Tomita S, Nakazawa M, Saga Y, Johnson RL. Mouse hesr1 and hesr2 genes are redundantly required to mediate Notch signaling in the developing cardiovascular system. Dev Biol. 2005; 278:301–9. [PubMed: 15680351]
49. Kokubo H, Tomita-Miyagawa S, Hamada Y, Saga Y. Hesr1 and Hesr2 regulate atrioventricular boundary formation in the developing heart through the repression of Tbx2. Development. 2007; 134:747–55. [PubMed: 17259303]

50. Sharff KA, Song WX, Luo X, Tang N, Luo J, Chen J, et al. Hey1 basic helix-loop-helix protein plays an important role in mediating BMP9-induced osteogenic differentiation of mesenchymal progenitor cells. J Biol Chem. 2009; 284:649–59. [PubMed: 18986983]
51. Salie R, Kneissel M, Vukevic M, Zamurovic N, Kramer I, Evans G, et al. Ubiquitous overexpression of Hey1 transcription factor leads to osteopenia and chondrocyte hypertrophy in bone. Bone. 2010; 46:680–94. [PubMed: 19857617]
52. Fischer A, Steidl C, Wagner TU, Lang E, Jakob PM, Friedl P, et al. Combined loss of Hey1 and HeyL causes congenital heart defects because of impaired epithelial to mesenchymal transition. Circ Res. 2007; 100:856–63. [PubMed: 17303760]
53. Luna-Zurita L, Prados B, Grego-Bessa J, Luxan G, del Monte G, Benguria A, et al. Integration of a Notch-dependent mesenchymal gene program and Bmp2-driven cell invasiveness regulates murine cardiac valve formation. J Clin Invest. 2010; 120:3493–507. [PubMed: 20890042]
54. Mann CD, Bastianpillai C, Neal CP, Masood MM, Jones DJ, Teichert F, et al. Notch3 and HEY-1 as prognostic biomarkers in pancreatic adenocarcinoma. PLoS One. 2012; 7:e51119. [PubMed: 23226563]
55. Candy PA, Phillips MR, Redfern AD, Colley SM, Davidson JA, Stuart LM, et al. Notch-induced transcription factors are predictive of survival and 5-fluorouracil response in colorectal cancer patients. Br J Cancer. 2013; 109:1023–30. [PubMed: 23900217]
56. Forghanifard MM, Taleb S, Abbaszadegan MR. Notch Signaling Target Genes are Directly Correlated to Esophageal Squamous Cell Carcinoma Tumorigenesis. Pathol Oncol Res. 2015; 21:463–7. [PubMed: 25361534]
57. Jung CW, Kong JS, Seol H, Park S, Koh JS, Lee SS, et al. Expression of activated Notch1 and HEY1 in papillary thyroid carcinoma. Histopathology. 2016
58. Tsuru A, Setoguchi T, Matsunoshita Y, Nagao-Kitamoto H, Nagano S, Yokouchi M, et al. Hairy/enhancer-of-split related with YRPW motif protein 1 promotes osteosarcoma metastasis via matrix metallopeptidase 9 expression. Br J Cancer. 2015; 112:1232–40. [PubMed: 25742474]
59. Hume CR, Bratt DL, Oesterle EC. Expression of LHX3 and SOX2 during mouse inner ear development. Gene Expr Patterns. 2007; 7:798–807. [PubMed: 17604700]
60. Lim YC, Oh SY, Cha YY, Kim SH, Jin X, Kim H. Cancer stem cell traits in squamospheres derived from primary head and neck squamous cell carcinomas. Oral Oncol. 2011; 47:83–91. [PubMed: 21167769]
61. Benito-Gonzalez A, Doetzlhofer A. Hey1 and Hey2 control the spatial and temporal pattern of mammalian auditory hair cell differentiation downstream of Hedgehog signaling. J Neurosci. 2014; 34:12865–76. [PubMed: 25232121]
62. Neves J, Parada C, Chamizo M, Giraldez F. Jagged 1 regulates the restriction of Sox2 expression in the developing chicken inner ear: a mechanism for sensory organ specification. Development. 2011; 138:735–44. [PubMed: 21266409]
63. Zhu X, Tollkuhn J, Taylor H, Rosenfeld MG. Notch-Dependent Pituitary SOX2(+) Stem Cells Exhibit a Timed Functional Extinction in Regulation of the Postnatal Gland. Stem Cell Reports. 2015; 5:1196–209. [PubMed: 26651607]
64. Smith A, Teknos TN, Pan Q. Epithelial to mesenchymal transition in head and neck squamous cell carcinoma. Oral Oncol. 2013; 49:287–92. [PubMed: 23182398]
65. Simões Bruno M, O'Brien Ciara S, Eyre R, Silva A, Yu L, Sarmiento-Castro A, et al. Anti-estrogen Resistance in Human Breast Tumors Is Driven by JAG1-NOTCH4-Dependent Cancer Stem Cell Activity. Cell Reports. 2015; 12:1968–77. [PubMed: 26387946]
66. Singh A, Settleman J. EMT, cancer stem cells and drug resistance: an emerging axis of evil in the war on cancer. Oncogene. 2010; 29:4741–51. [PubMed: 20531305]
67. Fukusumi T, Ishii H, Konno M, Yasui T, Nakahara S, Takenaka Y, et al. CD10 as a novel marker of therapeutic resistance and cancer stem cells in head and neck squamous cell carcinoma. Br J Cancer. 2014; 111:506–14. [PubMed: 24874475]
68. Prince ME, Sivanandan R, Kaczorowski A, Wolf GT, Kaplan MJ, Dalerba P, et al. Identification of a subpopulation of cells with cancer stem cell properties in head and neck squamous cell carcinoma. Proc Natl Acad Sci U S A. 2007; 104:973–8. [PubMed: 17210912]

69. Chen YC, Chen YW, Hsu HS, Tseng LM, Huang PI, Lu KH, et al. Aldehyde dehydrogenase 1 is a putative marker for cancer stem cells in head and neck squamous cancer. Biochem Biophys Res Commun. 2009; 385:307–13. [PubMed: 19450560]

70. Young MJ, Wu YH, Chiu WT, Weng TY, Huang YF, Chou CY. All-trans retinoic acid downregulates ALDH1-mediated stemness and inhibits tumour formation in ovarian cancer cells. Carcinogenesis. 2015; 36:498–507. [PubMed: 25742746]

71. Mirghani H, Ugolin N, Ory C, Goislard M, Lefevre M, Baulande S, et al. Comparative analysis of micro-RNAs in human papillomavirus-positive versus -negative oropharyngeal cancers. Head Neck. 2016; 38:1634–42. [PubMed: 27097597]

72. Suarez E, Gonzalez L, Perez-Mitchell C, Ortiz AP, Ramirez-Sola M, Acosta J, et al. Pathway Analysis using Gene-expression Profiles of HPV-positive and HPV-negative Oropharyngeal Cancer Patients in a Hispanic Population: Methodological Procedures. P R Health Sci J. 2016; 35:3–8. [PubMed: 26932277]

73. Fakhry C, Westra WH, Li S, Cmelak A, Ridge JA, Pinto H, et al. Improved survival of patients with human papillomavirus-positive head and neck squamous cell carcinoma in a prospective clinical trial. J Natl Cancer Inst. 2008; 100:261–9. [PubMed: 18270337]

STATEMENT OF TRANSLATIONAL RELEVANCE

The identification of HNSCC specific genes and pathways may be essential for targeted cancer therapy. Recently, several comprehensive genomic analyses reveal that the *NOTCH* pathway is closely related to HNSCC progression. However, defining which *NOTCH* pathway predominantly affects HNSCC development is not well examined and understood. In this study, we examined the role of *NOTCH4* using the TCGA data set and *in vitro* experiments. Consequently, we demonstrate that the *NOTCH4-HEY1* pathway is specifically up-regulated in HNSCC compared with normal tissue. We also demonstrate that *NOTCH4* promotes HNSCC proliferation, cisplatin resistance, a reduction in apoptosis and cell cycle alterations. Finally, we indicate that the *NOTCH4-HEY1* pathway promotes EMT by examining EMT-related genes such as *E-cadherin, Vimentin, Fibronectin, TWIST1* and *SOX2*. This finding has great potential for expanding our knowledge regarding the *NOTCH* pathway in cancer biology and may provide guidance in the development of novel specific HNSCC therapies.

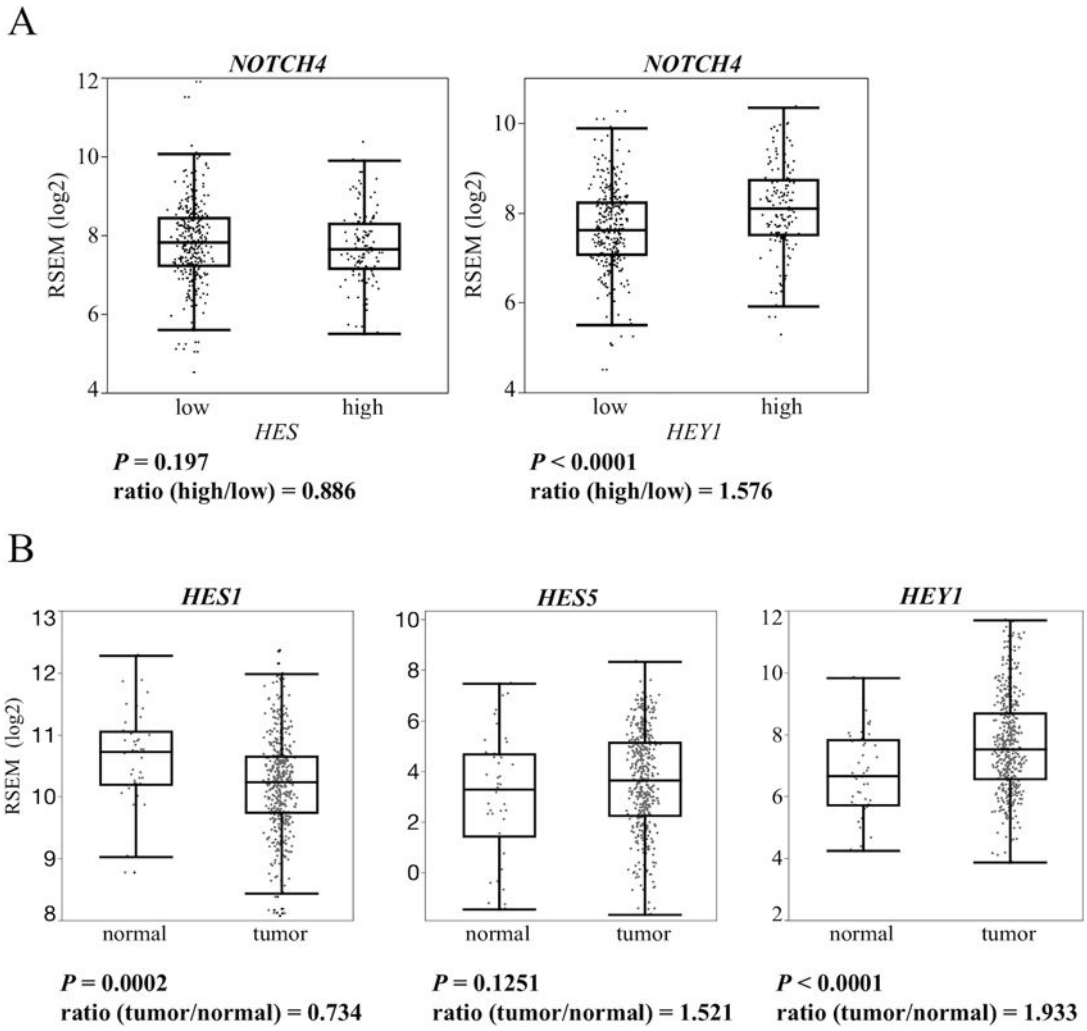

Figure 1. TCGA data set analysis of *HES/HEY* and *NOTCH4* relation

(A) *NOTCH4* expression is compared between the *HES* (*HES1+HES5*) and *HEY1* high/low group using the TCGA data set. Ratio is calculated by dividing the mRNA expression of the *HES* or *HEY1* high group by that of the low group. (B) *HES1, HES5* and *HEY1* expression are compared between HNSCC and normal tissue using the TCGA data set. Ratio is calculated by dividing the mRNA expression of the tumor samples by that of the normal samples. Whiskers indicate the minimum and maximum values. *P* value is calculated by using Student's *t*-test.

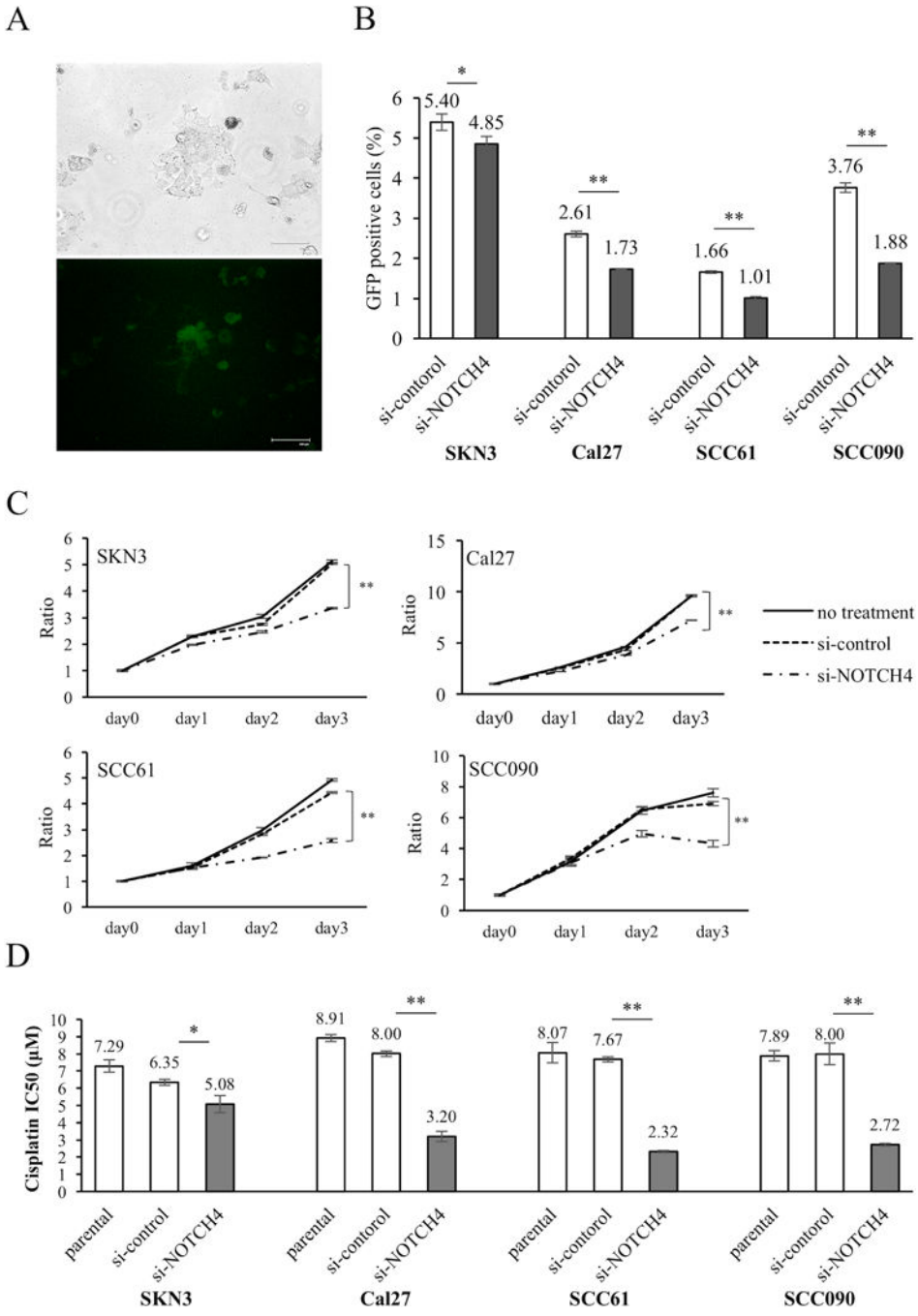

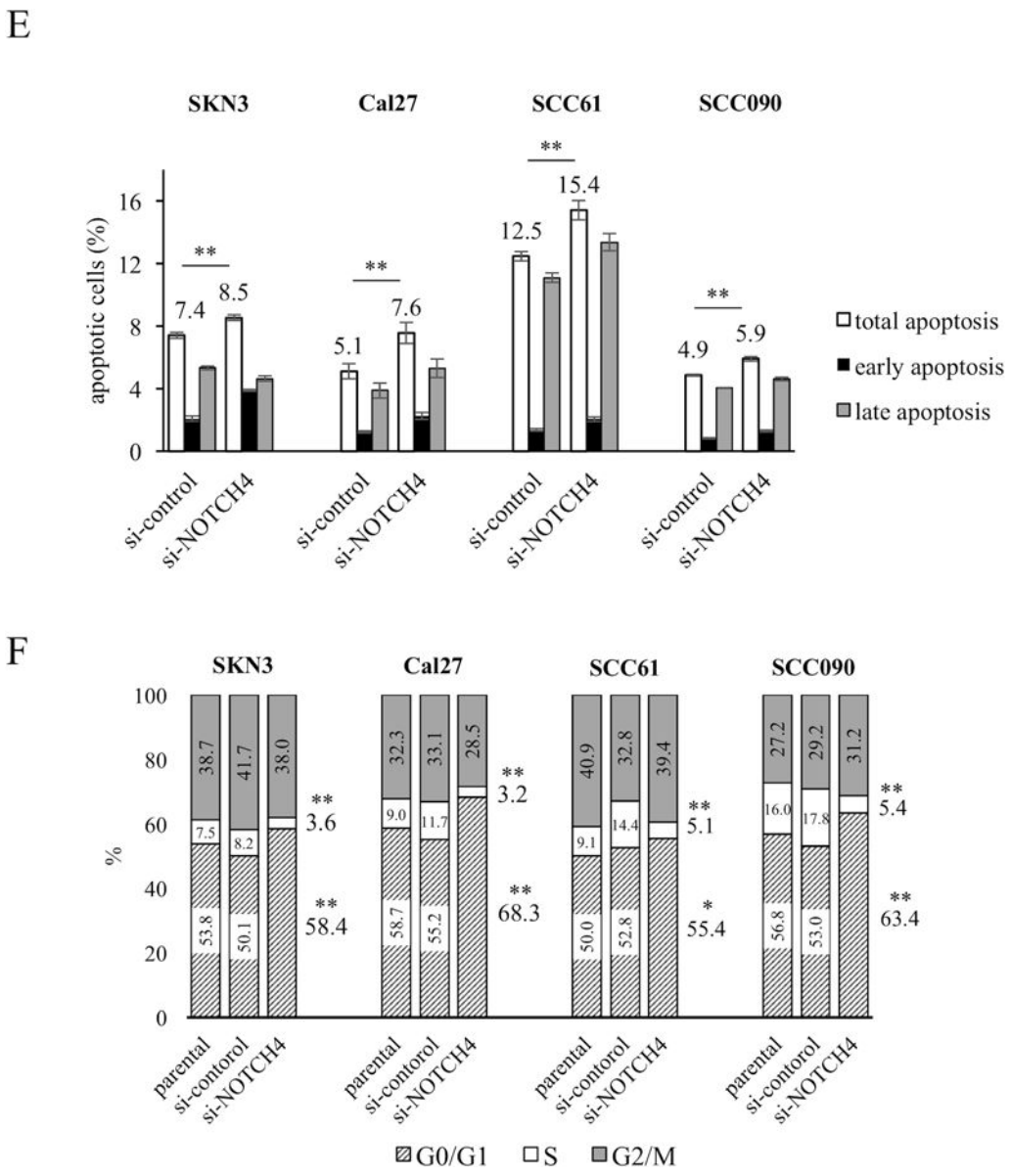

Figure 2. *NOTCH* activity, proliferation, cisplatin viability, apoptosis assay and cell cycle analysis of si-*NOTCH4* cells

(A) pGreenFire1-Notch plasmid vector was transfected to SKN3 cell. Scale bar indicates 100 μm. (B) *NOTCH* activity assay of si-control and si-*NOTCH4* cells. GFP positive cells have high *NOTCH* activity. (C) Proliferation assays. si-*NOTCH4* cells are compared cell growths to si-control cells on day 3. (D) IC50 of cisplatin in parental, si-control and si-*NOTCH4* cells. The IC50 differences between si-control and si-*NOTCH4* cells are compared. (E) Apoptosis assays. Total apoptotic fraction is defined as the sum of early and late apoptosis cells. (F) Cell cycle analysis. Each cell cycle phase is compared between si-control and si-*NOTCH4* cells. *P* value is calculated by using Student's *t*-test. *: $P < 0.05$, **: $P < 0.01$.

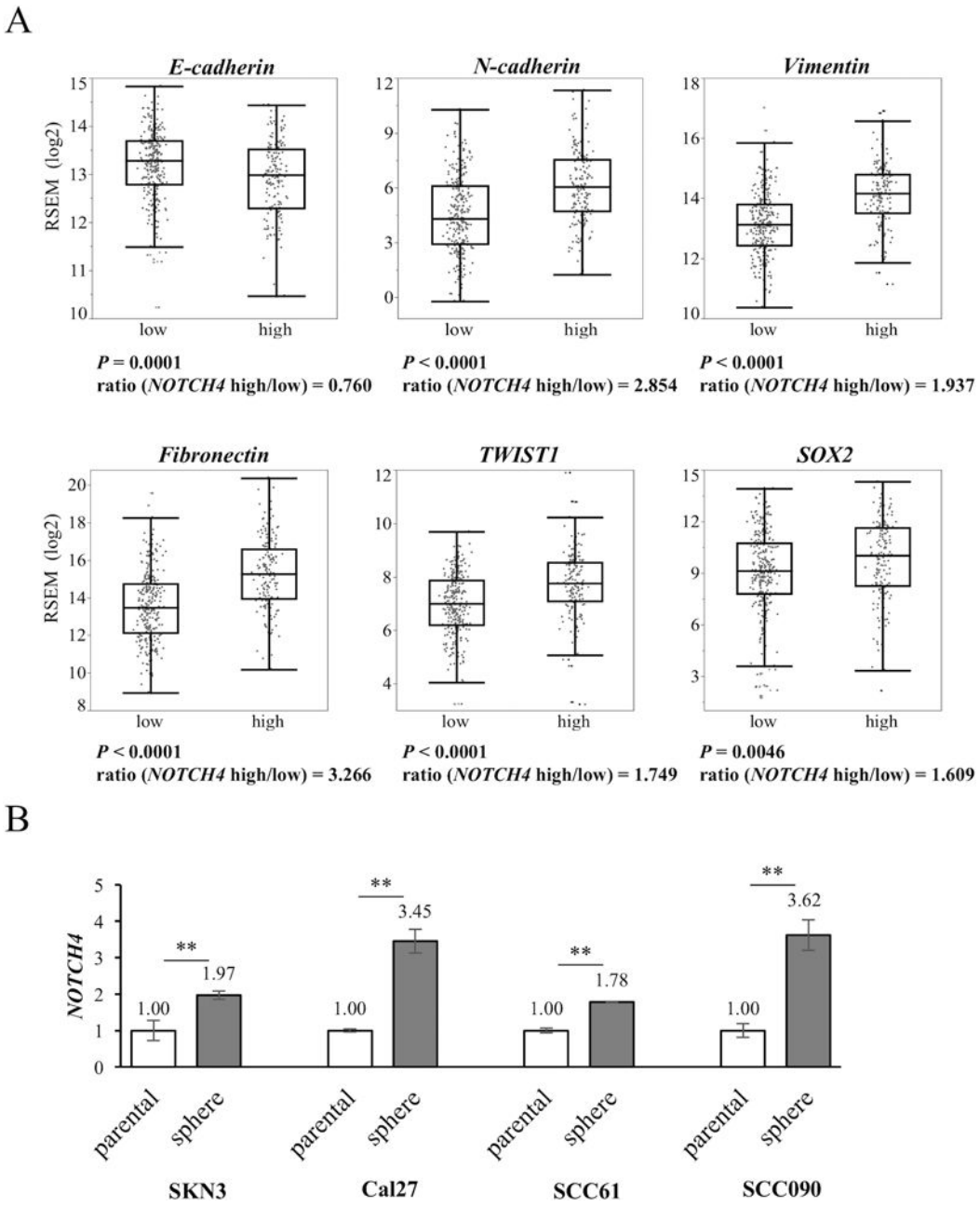

Figure 3. Comparison of EMT-related genes between the *NOTCH4* high and low groups using the TCGA data set. Comparison of *NOTCH4* expression between sphere and parental cells

(A) The *NOTCH4* high group is defined as tumors with expression 1 standard deviation greater than the mean of normal tissue for *NOTCH4*. The other tumors are defined as the low group. The boxes represent the interquartile range (25^{th}-75^{th}), and horizontal lines inside the boxes indicate the median. Whiskers indicate the minimum and maximum values. Ratio is calculated by dividing the mRNA expression of the high group by the expression of the low group. (B) *NOTCH4* expression is compared between parental and sphere cells using qRT-PCR. *P* value is calculated by using Student's *t*-test. **: $P < 0.01$.

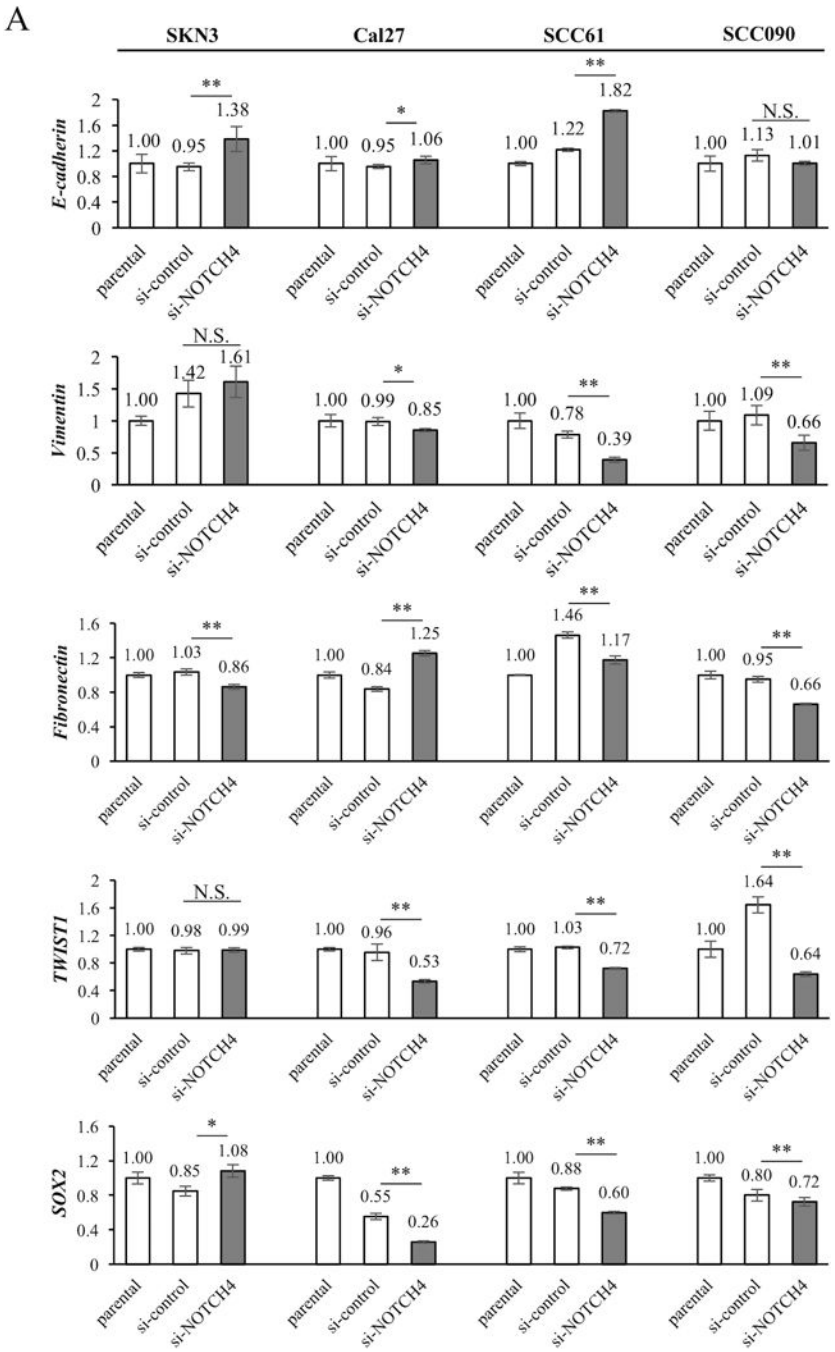

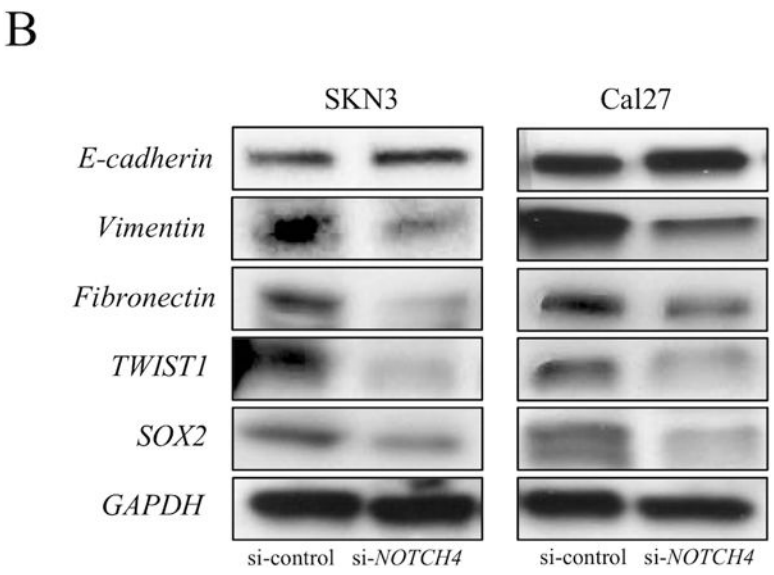

Figure 4. The expression of EMT-related genes in si-*NOTCH4* cells

(A) EMT-related gene (*E-cadherin, Vimentin, Fibronectin, TWIST1*, and *SOX2*) expression in parental, si-control and si-*NOTCH4* cells is measured by qRT-PCR. The expression differences between si-control and si-*NOTCH4* cells are compared. *P* value is calculated by using Student's *t*-test. *: $P < 0.05$, **: $P < 0.01$, N.S.: not significant. (B) Western blots of EMT-related genes in si-control and si-*NOTCH4* of SKN3 and Cal27 cells. *GAPDH* antibody is used as a control.

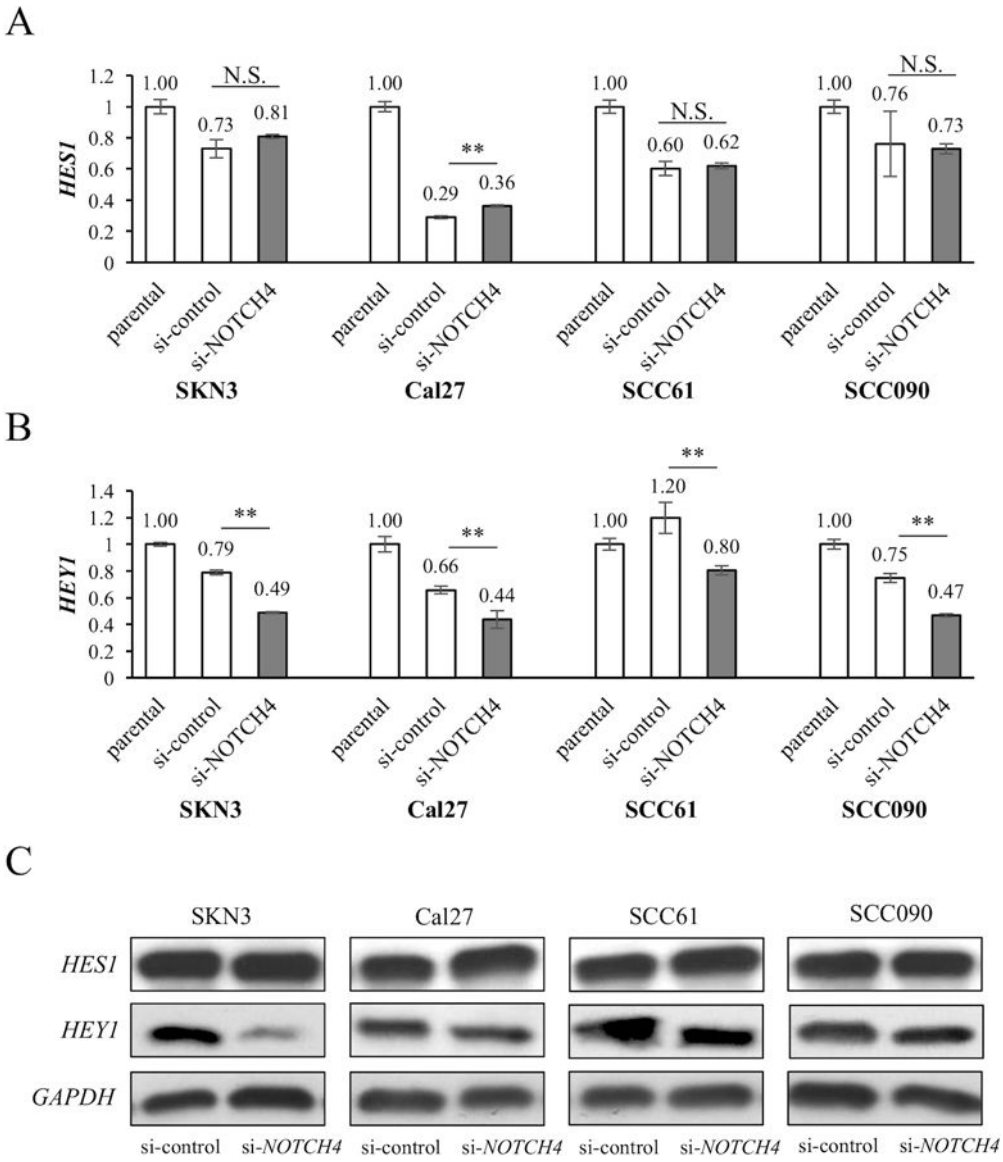

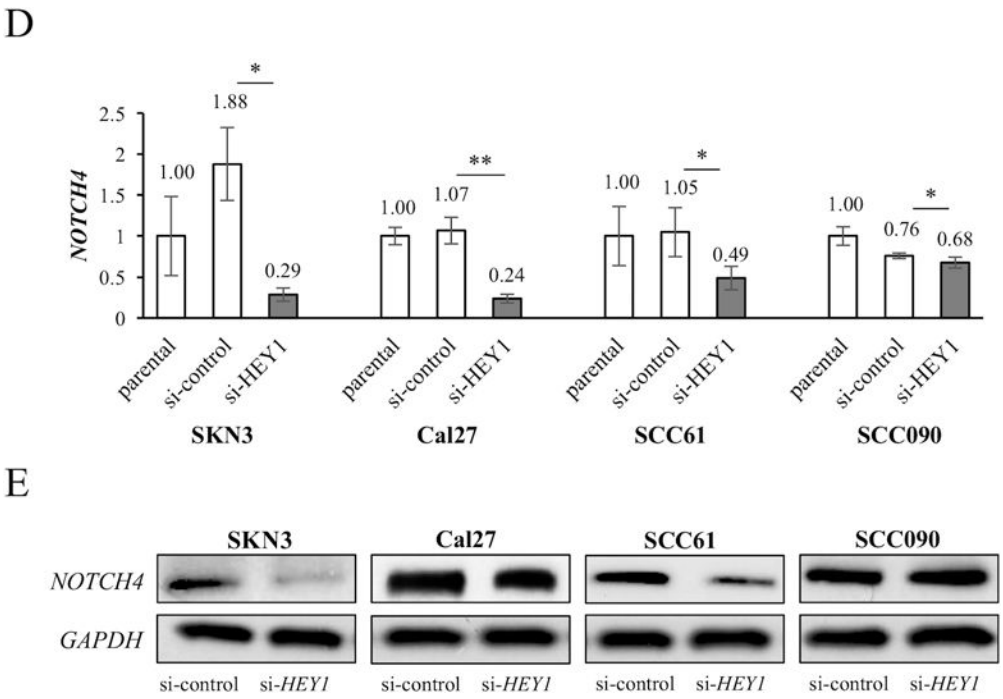

Figure 5. *HES1*/*HEY1* expression in si-*NOTCH4* cells and *NOTCH4* expression in si-*HEY1* cells

HES1 (A) and *HEY1* (B) expression in parental, si-control and si-*NOTCH4* cells. mRNA expression is measured by qRT-PCR. The expression differences between si-control and si-*NOTCH4* cells are compared. (C) Western blots of *HES1* and *HEY1* in si-control and si-*NOTCH4* cells. (D) *NOTCH4* expression of parental, si-control and si-*HEY1* cells. mRNA expression is measured by qRT-PCR. The expression differences between si-control and si-*HEY1* cells are compared. (E) Western blots of *NOTCH4* in si-control and si-*HEY1* cells. *GAPDH* antibody is used as a control. *P* value is calculated by using Student's *t*-test. *: $P < 0.05$, **: $P < 0.01$, N.S.: not significant.

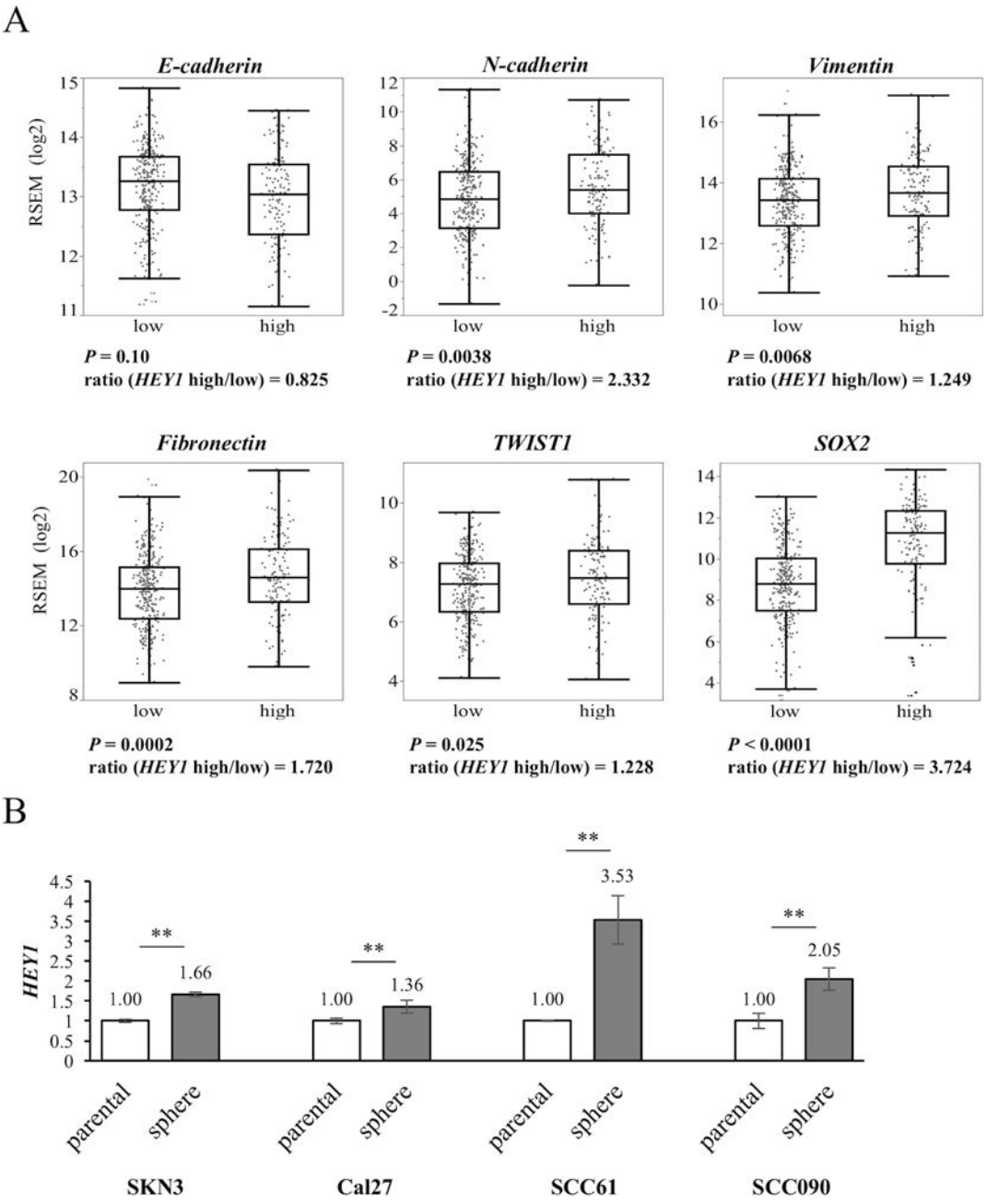

Figure 6. Comparison of *HEY1* and EMT-related genes using TCGA data set. Comparison of *HEY1* expression between sphere and parental cells

(A) Comparison of EMT-related genes between *HEY1* high and low groups using the TCGA data set. The boxes represent the interquartile range (25^{th}-75^{th}), and horizontal lines inside the boxes indicate median. Whiskers indicate the minimum and maximum values. Ratio is calculated by dividing the mRNA expression of the high group by the expression of the low group. (B) *HEY1* expression is compared between parental and sphere cells using qRT-PCR. *P* value is calculated by using Student's *t*-test. **: $P < 0.01$.

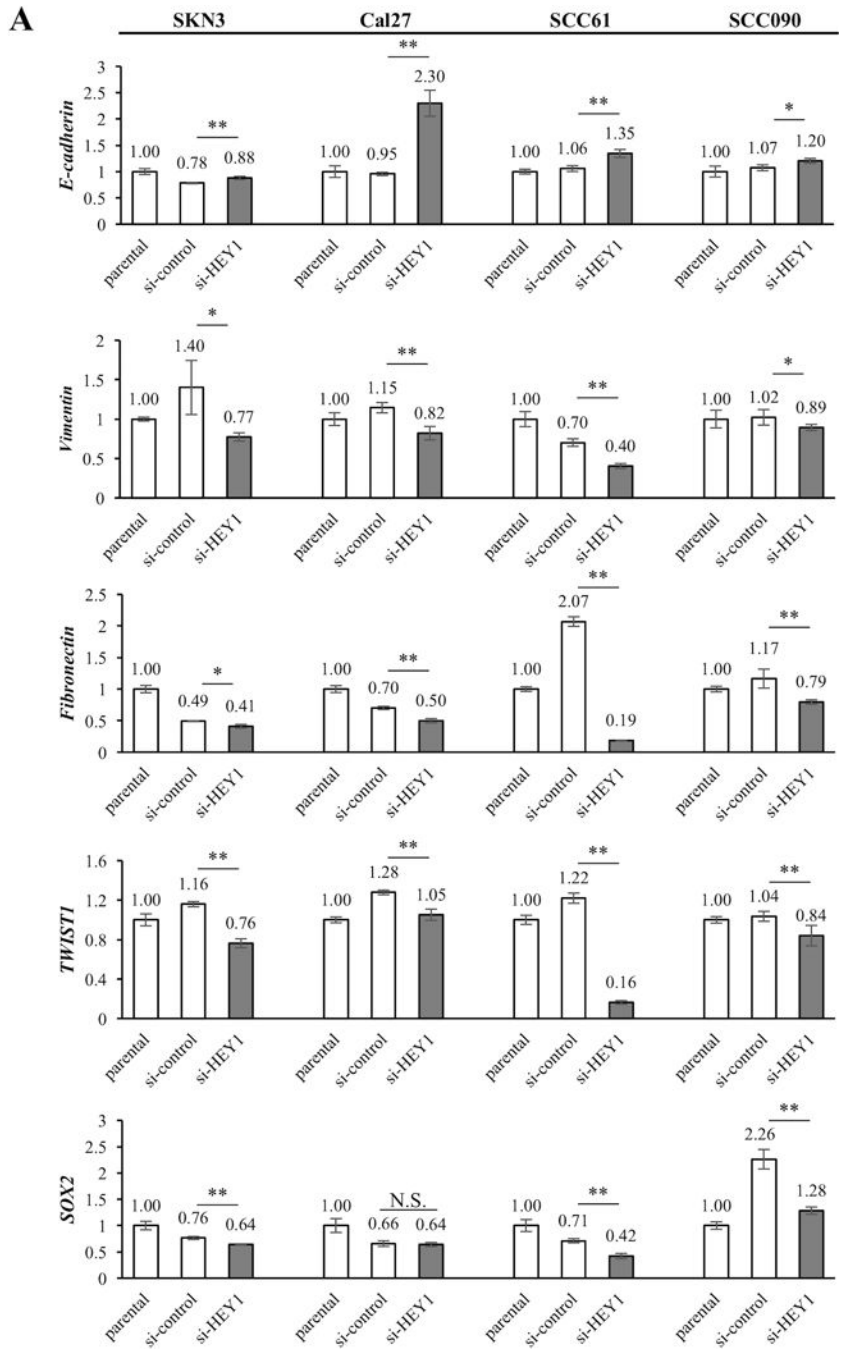

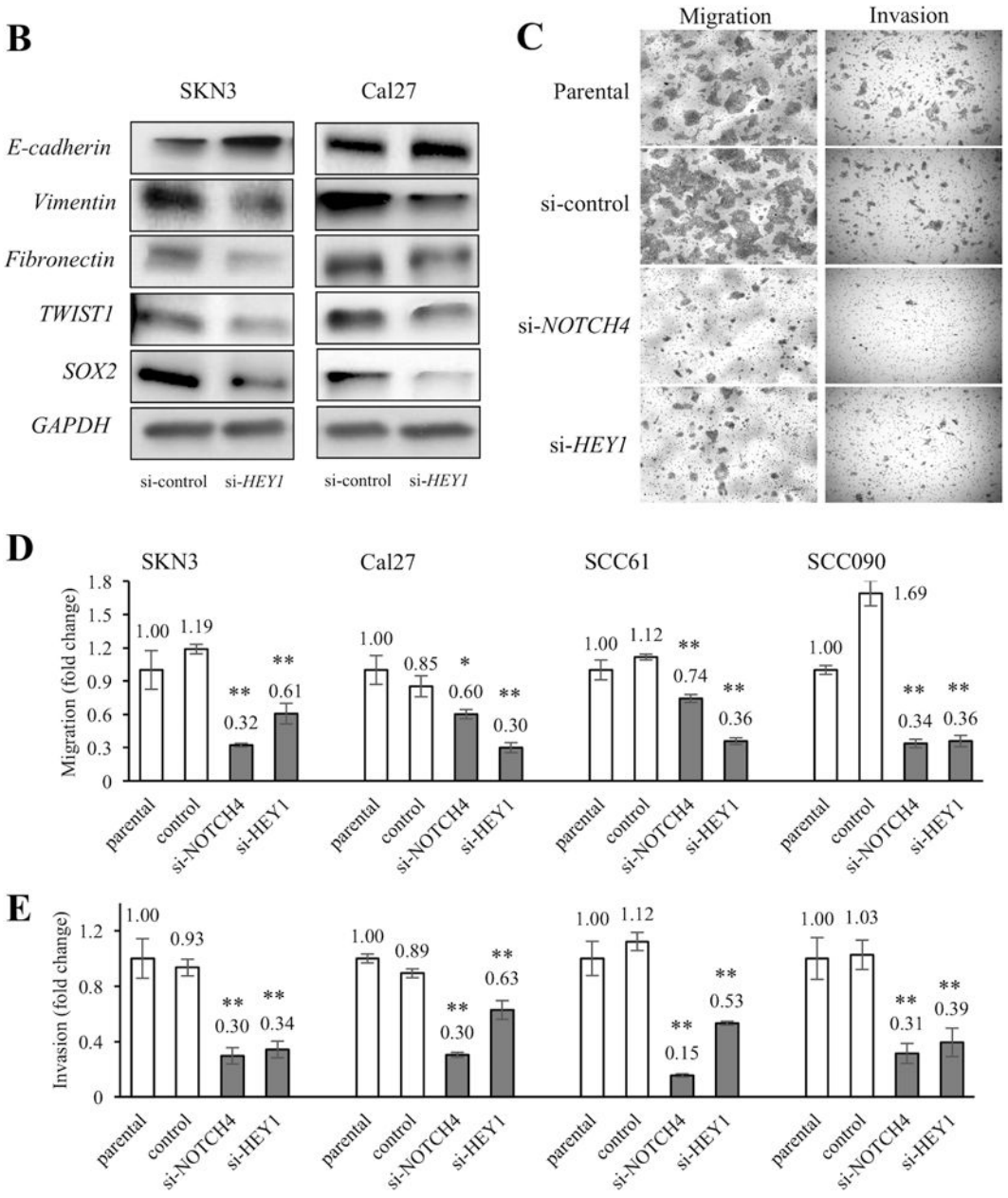

Figure 7. *HEY1* relates to EMT gene expression and EMT functions

(A) The comparisons of EMT-related gene (*E-cadherin, Vimentin, Fibronectin, TWIST1* and *SOX2*) expressions among parental, si-control and si-*HEY1* cells. The expression differences between si-control and si-*HEY1* cells are compared. (B) Western blots of EMT-related genes in si-control and si-*HEY1* cells. (C) Representative images of migration and invasion assays. The cell line is SCC090. (D, E) Migration and invasion assays in parental, si-control, si-*NOTCH4* and si-*HEY1* cells. The migration and invasion indexes were calculated by deviding the number of parental cells thorough the chamber. The differences between si-control and si-*NOTCH4*/si-*HEY1* cells are compared. *P* value is calculated by using Student's *t*-test. *: $P < 0.05$, **: $P < 0.01$, N.S.: not significant.